Journal of Alloys and Compounds 694 (2017) 710–714

Contents lists available at ScienceDirect

Journal of Alloys and Compounds

journal homepage: http://www.elsevier.com/locate/jalcom

Microcalorimetry: A powerful tool for quantitative analysis of aging hardening response of Cu-Ni-Sn alloys

E. Donoso [a], M.J. Diánez [b], A. Perejón [b, c], P.E. Sánchez-Jiménez [b], L.A. Pérez-Maqueda [b], M.J. Sayagués [b], J.M. Criado [b, *]

[a] Departamento de Ciencia de Materiales, Facultad de Ciencias Físicas y Matemáticas, Universidad de Chile, Casilla 2777, Santiago, Chile
[b] Instituto de Ciencia de Materiales de Sevilla, C.S.I.C., Centro Mixto Universidad de Sevilla-C.S.I.C., Américo Vespucio 49, Isla de La Cartuja, 41092, Sevilla, Spain
[c] Departamento de Química Inorgánica, Facultad de Química de la Universidad de Sevilla, Profesor García González 1, 41012, Sevilla, Spain

ARTICLE INFO

Article history:
Received 17 August 2016
Received in revised form
6 October 2016
Accepted 7 October 2016
Available online 8 October 2016

Keywords:
Aging
Alloys
Hardness
Differential Scanning Calorimetry (DSC)

ABSTRACT

The method for the deconvolution of overlapping DSC peaks here proposed has been used by the first time for the quantitative determination of the enthalpies associated to the phase transitions undergone during the aging of an alloy. They have been determined the enthalpies evolved along the first and the second overlapping DSC traces of Cu-10 wt%Ni-5.5 wt%Sn alloy, which are associated, respectively, to the spinodal decomposition of the alloy and the segregation of a DO_{22} $(Cu_xNi_{1-x})_3Sn$ tetragonal phase. The fraction of the DO_{22} phase (responsible of the aging hardening of this alloy) has been successfully determined from DSC as a function of the annealing treatment, while TEM and XRD failed for this purpose. It has been demonstrated that a threshold higher than 50% of crystallization of the DO_{22} phase is required for achieving a significant increase of the hardness as a function of the crystallization percentage. These results suggest that microcalorimetric measurement can be a powerful tool to establish quantitative relationships between the mechanical, electrical or functional properties of alloys and their structural changes undergone by aging.

1. Introduction

There is currently a great industrial interest in developing materials with both a large thermal/electrical conductivity and a very high toughness. Metal alloys that can be strengthened by aging are the best candidates for this purpose, which explain the large number of papers on this topic appeared in recent literature [1–7]. The improvement of the mechanical properties of the alloys by aging is due to the formation of new phases during the annealing treatment that hinder the atomic movement of the bulk. The structural characterization of these phases is generally carried out by combining Transmission Electron Microscopy (TEM) or High Resolution Electron Microscopy (HRTEM) with Electron Diffraction (ED). It is noteworthy to point out that TEM and ED have lead very often to a successfully identification of the phases responsible of the hardening by aging. However, these methods do not allow a quantitative determination of the percentage of the new phases formed as a function of the aging time. Moreover, X-ray diffraction generally cannot be used for this purpose because the percentages of the new phases formed in the bulk alloy are too low for being detected by this procedure [8,9]. Differential Scanning Microcalorimetry (DSC) has been successfully used in literature [10–16] for discriminating the successive phase transitions taking place as a function of the aging temperature. Esmaeili et al. [17] have used enthalpies measurements from DSC for estimating the relative volume of precipitates formed by aging an Al-Mg-Si-Cu alloy AA6111 in order to get a quantitative relationship between this parameter and the strengthening of the alloy by aging. They [17] calculated the relative volume of precipitates from the total enthalpy corresponding to the whole set of overlapping DSC peaks associated to the successive phase transitions undergone by the AA6111 alloy. The discrimination of the real enthalpies evolved by every one of the individual processes that are overlapping would allow a quantitative determination of the enthalpy change associated to the phase transition really responsible of the alloy strengthening.

* Corresponding author. Instituto de Ciencia de Materiales de Sevilla (C.S.I.C.-Univ. Sevilla), C. Américo Vespucio 49, Sevilla, 41092, Spain.
E-mail address: jmcriado@icmse.csic.es (J.M. Criado).

http://dx.doi.org/10.1016/j.jallcom.2016.10.060
0925-8388/

Cu-Ni-Sn alloys in the copper reach region of the ternary phase diagram are widely used in the electronics, automotive and aerospace industry [18] because they combine high electrical conductivity, corrosion resistance and hardness. It has been shown in literature [19–23] that these alloys undergo a dramatic improvement in their mechanical properties by aging at temperatures ranging from 200 °C up to 400-450 °C. This behavior has been attributed either to a spinodal decomposition of the alloy in two phases; Sn reach and Sn lean, respectively, or to the $(Cu_xNi_{1-x})_3Sn$ DO_{22} phase grown from the Sn reach one resulting from the spinodal decomposition. We have shown in a paper recently published in this journal [24] that DSC allows discriminating the annealing temperature regions of the spinodal decomposition and the segregation of the DO_{22} phase coherent within the alloy matrix with composition Cu-10 wt%Ni-5.5 wt%Sn. Fig. 1 has been composed for summarizing the results previously reported [24] by us for the transformations undergone by this alloy as a function of the annealing temperature. This figure clearly shows the two overlapping peaks associated to the spinodal decomposition and the segregation of the DO_{22} phase, respectively, as well as the Electron Diffraction Patterns associated to both structures as shown in Ref. [24]. They agree with the fcc structure expected for a spinodal decomposition and the tetragonal lattice corresponding to the $(Cu_xNi_{1-x})_3Sn$ DO_{22} phase, respectively. It is noteworthy to point out that the DO_{22} phase was observed from TEM analysis of the samples annealed at temperatures ranging from 200 °C to 450 °C, which suggest that no metastable phases different to the DO_{22} one were formed along the second DSC peak in Fig. 1. Moreover, the values of the Vicker microhardness that were measured in Ref. [24] at the temperatures marked with arrows on Fig. 1 clearly demonstrated that the improvement of the mechanical properties of this alloy by aging lies exclusively on the formation of a DO_{22} phase.

Cu-Ni-Sn alloys could be a proper system for checking the power of DSC for discriminating the enthalpies associated to overlapping phase transitions. A DSC analysis of previously annealed samples could allow determining the relationship between the crystallization fraction of the phase responsible of the strengthening of the alloy and its corresponding hardness, leading to a better understanding of the hardening mechanism.

The scope of the present work is determining the correlation between the enthalpy of the DO_{22} transition phase of Cu-10 wt%Ni-5.5Sn samples submitted at different aging treatments and the hardness of the sample.

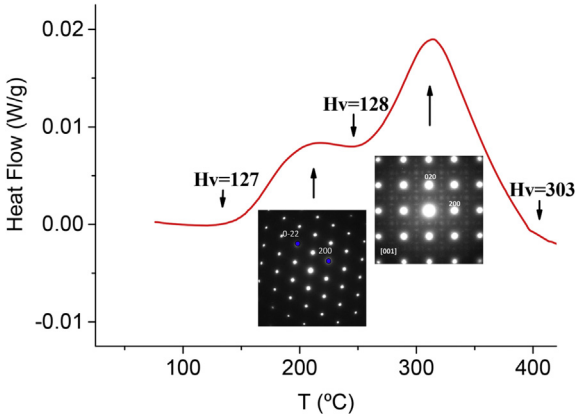

Fig. 1. DSC, Electron Diffraction patterns (EDP) associated the phase formed in the first and second DSC step, respectively, and microhardnes measured at the annealing temperatures marked with arrows.

2. Experimental

The starting alloy was prepared by melting a stoichiometric mixture of copper, nickel and tin of high purity in an induction furnace under argon atmosphere and submitted to the successive annealing and cold rolling treatments for achieving complete homogenization before being water quenched at room temperature for preserving the α-Cu structure of the homogeneous supersaturates solid solution, as described in Ref. [24].

A Differential Scanning Calorimeter from TA Instruments, model Q 200 was used. The DSC diagrams were recorded under a flow of nitrogen of 100 cc/min. A disc of pure copper was used as reference material for minimizing the deviation of the base line. The base line was recorded using pure copper both as reference and sample material under the same experimental conditions used for recording the DSC plot to be corrected.

Vicker microhardness measurements were carried out at room temperature in a Futur-Tech FM-700 microdurometer employing a load of 2 N during 10 s. Each microhardness value was calculated as an average of 5 indentations.

3. Results

It is evident that the enthalpy calculated from the DSC of an aged sample would be associated to the fraction of the new phase that was not yet segregated from the alloy during the annealing treatment. Thus, a comparison with the transition enthalpy of the corresponding sample that has not been annealed would allow determining the fraction of the phase responsible of the hardening that has really crystallized during the annealing treatment.

The enthalpy associated to a given DSC curve can be directly determined for the total area enclosed between the curve and the base line according with the following expression:

$$\Delta H = \int_0^t \frac{d\Delta H}{dt} dt = A_t \tag{1}$$

ΔH being the reaction enthalpy; t, the time; $d\Delta H/dt$, the variation of the enthalpy per unit time, represented by the heat flow in the DSC diagrams, and A_t is the area enclosed by the DSC curve.

Equation (1) applies if the DSC plot were represented as a function of the time. However, the standardized procedure of representing these diagrams implies to plot the evolved energy per unit time as a function of temperature. Thus, if we take into account that DSC are recorded at a constant heating rate $\beta = dT/dt$, Equation (1) becomes:

$$\Delta H = A_t = \frac{A_T}{\beta} \tag{2}$$

where A_T is the area of the DSC peak if represented as a function of the temperature.

The value of ΔH determined from Equation (2) must be independent of the heating rate used for obtaining the DSC plots. Thus, a set of DSC traces of the non-annealed Cu-10 wt%Ni-5.5Sn alloy have been recorded at heating rates ranging from 10 °C/min up to 40°C/min in order to check the accuracy of the enthalpies determined from calorimetric measurements. The results obtained are shown in Fig. 2.

The calculation of the enthalpies associated to the two overlapping phase transitions observed in Fig. 2 would require the previous deconvolution of the corresponding two overlapping exothermic peaks. It has been demonstrated in previous papers [25–27] that the Fraser-Suzuky function allows the deconvolution

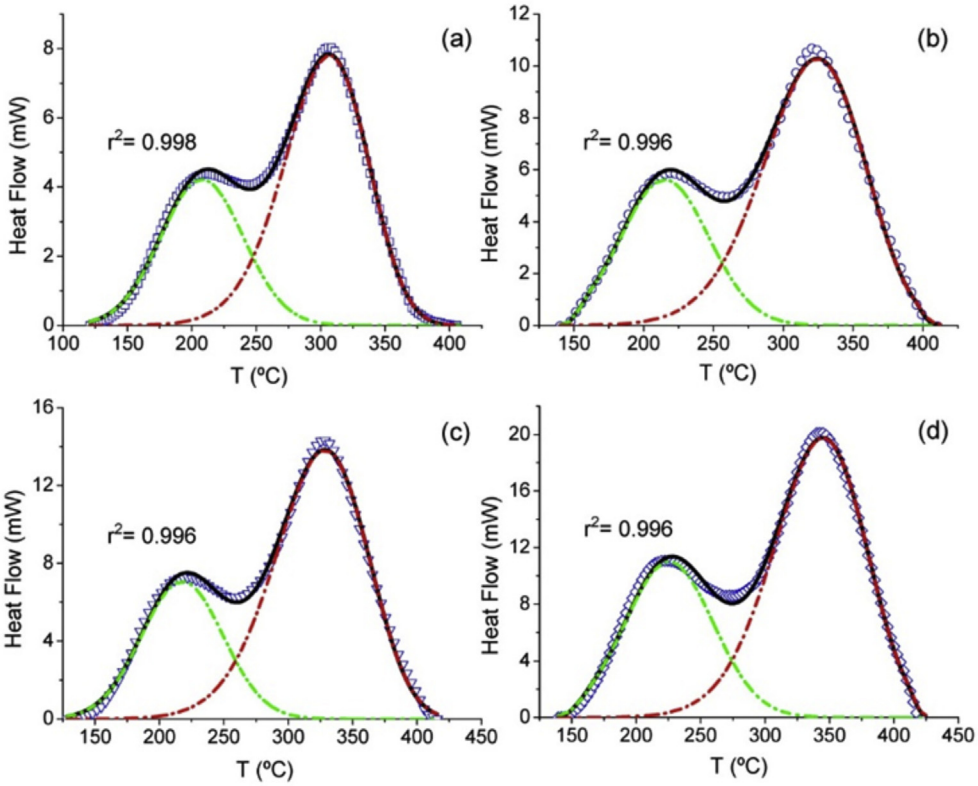

Fig. 2. Experimental DSC curves (dots) obtained at heating rates of 10 °C/min (a), 15 °C/min (b), 20 °C/min (c) and 30°C/min (d) for the non-annealed Cu-10%Ni-5.5%Sn alloy and plots resulting from the deconvolution of the two overlapping peaks by means of Fraser-Suzuki functions whose overlay fits the experimental DSC curves (solid line).

of overlapping thermal analysis peaks with a great precision because it is not associated to a predefined symmetry (like Gauss Pearson VII, etc., functions) and, therefore, it can fit the real curves whatever would be their shape, which is strongly dependent on the phase transition kinetics. The results obtained for the deconvolution of the overlapping DSC peaks by means of the Frazer-Suzuky function are also shown in Fig. 2 together with the regression coefficients obtained.

It is noteworthy to point out that the enthalpies obtained from Equation (2) for the first and second DSC peaks, after considering the corresponding areas resulting from the deconvolution shown in Fig. 2, are independent of the heating rate used, which corroborate the validity of the deconvolution method here used. The enthalpy determined from the first DSC peak attributed to the spinodal decomposition of the Cu-9wt% Ni- 5.5 wt% Sn alloy has been equal to 7.7 ± 0.2 J/g, while the enthalpy of the second DSC peak corresponding to the formation of a $(Cu_xNi_{1-x})_3Sn$ coherent with the alloy matrix has been equal to 13.1 ± 0.3 J/g.

DSC would allow determining the phase percentage that has crystallized during the annealing treatment of the alloy. This is because the enthalpy determined from the DSC of the aged sample should be proportional to the phase fraction that had not yet crystallized during the previous annealing treatment and, therefore, will crystallize during the subsequent DSC run. Thus, the microcalorimetric analysis would allow determining the relationship between the crystallized fraction and the measured hardness of the alloy provided that the new phase formed is responsible of the improvement of the alloy mechanical properties.

Fig. 3 shows the DSC obtained for the Cu-9wt%Ni-5.5%Sn after being submitted to different aging treatments. It can be observed that the first DSC peak, attributed to the spinodal decomposition, disappears by annealing the sample at temperature higher than

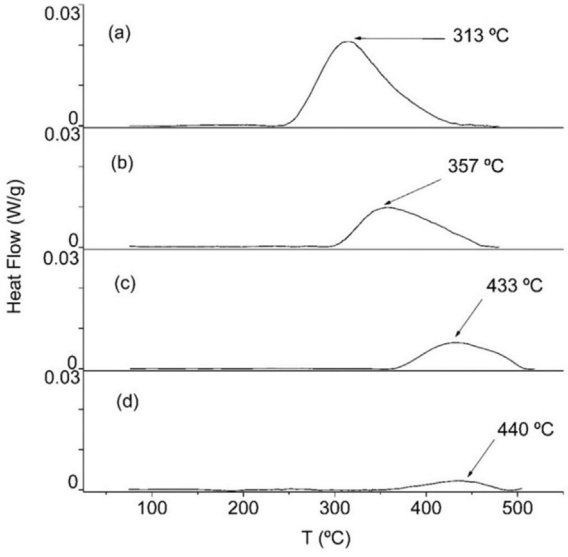

Fig. 3. DSC diagrams recorded at a heating rate of 10°C/min for Cu-10%Ni-5.5%Sn samples previously annealed for 2 h at temperatures of 200 °C (a), 250 °C (b), 300 °C (c) and 350 °C (d), respectively, and at 450 °C for 45 min.

200 °C. Thus, the DSC peaks recorded on Fig. 3 would correspond to the crystallization of the DO_{22} phase that had not yet crystallized along the aging treatments and, therefore, crystallizes after the subsequent DSC run. The percentage of the DO_{22} phase that had not yet crystallized during the annealing treatment would be obtained from the ratio between the enthalpy determined from the area of

the DSC curve of the sample aged at the temperature T, ΔH_T, and the total enthalpy determined from the non-annealed sample, ΔH_t (=13.1 J/g). The percentage, W_T%, of the DO_{22} phase crystallized after aging the alloy at the temperature T is given by the following equation:

$$W_T(\%) = \left(1 - \frac{\Delta H_T}{\Delta H_t}\right) \cdot 100 \quad (3)$$

It is noteworthy to point out that the temperature of the DSC peaks shown in Fig. 3 increases by increasing the previous annealing temperature of the sample. This behavior can be explained if we take into account that, for kinetic reasons, the DSC plots moves to higher temperatures as far as the initial conversion increases. The W_T values obtained after aging the Cu-10 wt%Ni-5.5 wt%Sn alloy for 2 h at temperatures ranging from 200 °C to 450 °C are included in Table 1 together with the corresponding values measured for the Vicker hardness.

The plot of the Vicker hardness as a function of the percentage of DO_{22} phase crystallized because of the aging treatment is shown in Fig. 4. These results clearly show that the strengthening of the Cu-10 wt%Ni-5.5 wt%Sn is not directly proportional to the percentage of DO_{22} phase crystallized, but it is necessary to reach a threshold higher that 50% of crystallization before achieving a dramatic increase of the hardness as a function of the crystallization percentage. In order to explain this behavior it would be necessary to consider the possible influence on the alloy hardness of both the crystal size and the relative volume fraction of the DO_{22} phase segregated as a function of the annealing treatment. It has been shown in literature [28,29] that the aging strengthening of alloys could be promoted by the segregation of nanosized particles, leading to an improvement of the mechanical properties as the crystal size decreases. Thus, in the case of a significant influence of the DO_{22} crystal size on the alloy strengthening, the hardness values obtained at lower annealing temperatures should be higher than the expected just from the contribution of the DO_{22} relative volume fraction, contrarily to the behavior reported in Table 1 and Fig. 4. This is because the crystal growth rate increases exponentially with the temperature and, therefore, smaller crystal sizes of the DO_{22} phase would be generated at lower temperatures. Thus, the relationship found between the Vicker hardness and the relative volume fraction of the DO_{22} phase cannot be explained by assuming a contribution of the crystal size to the hardness. These considerations suggest that the correlation between the hardness of the Cu-10 wt%Ni-5.5 wt%Sn alloy and the annealing temperature is exclusively due to the contribution of the percentage of DO_{22} phase segregated from the alloy bulk. This conclusion would be supported by the results obtained by us from the study of precipitation hardening of a set of copper alloys in the copper reach region of the corresponding phase diagrams. It was reported [11,30] that the maximum value attained by the hardness of the alloy was independent of the annealing temperature in the temperature range at which the formation of the phase responsible of the aging hardening occurs. It can be concluded from these results that the mechanical properties of these alloys [11,30] were not influenced by the crystal size of the precipitates. This conclusion can be supported by considering that the crystal size growth rate increases by increasing the annealing temperature and/or time, while the maximum concentration of the segregated phase is only depending on the alloy composition. On the other hand, it is noteworthy to point out that the Vicker microhardness measured after annealing the Cu-10 wt%Ni-5.5 wt%Sn sample for 80 min was equal to 310 ± 9. The good agreement between this value and the one reported in Table 1 for the sample annealed for 2 h show that the alloy hardness is independent of the annealing time in the above time range, which supports the lack of influence of the crystal size of the DO_{22} phase on the hardening response.

The results obtained could be explained by considering that the interaction between neighbor DO_{22} nanocrystals embedded into the bulk α-Cu phase would be required either for hindering the atomic movement or for the anchorage of the dislocations that would be generated during the quenching for obtaining the Cu-10% Ni-5.5Sn supersaturated solid solution. Thus, a DO_{22} concentration threshold would be required for achieving the crystal interaction.

Finally, it is noteworthy to point out that, although the new phases formed as a function of the annealing temperature of an alloy can be identified by TEM or HRTEM, it is not possible the quantitative determination of the crystallized fraction from these techniques. Moreover, X- ray diffraction seldom can be used for this purpose because, like occurs in our case [24], the percentage of the new phases formed is generally too low for being detected from XRD.

Table 1
Vicker microhardness (H_v), Enthalpies (ΔH_a) calculated from Fig. 3 and crystallization percentages (X_T) of the DO_{22} phase as a function of annealing temperature (T).

T (°C)	ΔH_T (J/g)	W_T (%)	H_v
Non-annealed[a]	13,1 ± 0.3	0	117 ± 8
200	11,0 ± 0.1	16 ± 2	128 ± 5
250	5,7 ± 0.2	56 ± 3	146 ± 5
300	3,4 ± 0.2	74 ± 5	256 ± 8
350	1,3 ± 0.3	90 ± 6	312 ± 6
450[b]	0	100	303 ± 7

[a] $\Delta H_T = \Delta H_t$ for the starting sample prepared by quenching.
[b] No DSC peak was observed in this case.

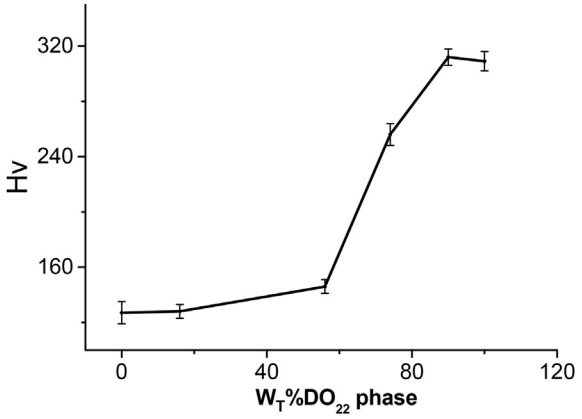

Fig. 4. Relationships between the microhardness of Cu-10%Ni-5.5%Sn alloy and the fraction of the DO_{22} phase segregated after several annealing treatments.

4. Conclusions

The deconvolution method of DSC peaks here outlined has allowed to determine the enthalpies of the two overlapping exothermic peaks of the Cu-10 wt%Ni-5.5 wt%Sn alloy, associated to the spinodal decomposition of the alloy and the segregation of a DO_{22} phase (responsible of the strengthening of the alloy), respectively. A correlation between the percentage of crystallization of the DO_{22} phase and the strengthening of the alloy has been obtained from enthalpies and hardness measurements as a function of the annealing time. A crystallization threshold higher than 50% is required for significantly improving the mechanical properties of the alloy.

Acknowledgement

The authors would like to acknowledge the facilities provided by the Instituto de Ciencia de Materiales de Sevilla (Spain) and the Departamento de Ciencia de Materiales of the University of Chile (Chile). One of us (A. Perejón) also thank VPPI-US for the AP current contract. Financial support by projects CTQ2014-52763-C1–R (Ministerio de Economia y Competitividad, Spanish government-FEDER) and TEP-7858 (Junta de Andalucia-FEDER) is acknowledged.

References

[1] Q. Feng, L.N. Song, Y.W. Zheng, Y.T. Fang, L. Meng, J.B. Liu, H.T. Wang, L. Meng, J.B. Liu, H.T. Wang, Evolution of fcc/bcc interface and its effects on the strengthening of severe drawn Cu-3wt%Cr, J. Alloys Compnd. 640 (2015) 45–50.
[2] C.H. Liu, Y.X. Lai, J.H. Chen, G.H. Tao, L.M. Liu, P.P. Ma, C.L. Wu, Natural aging-induced reversal of the precipitation pathways in an Al-Mg-Si alloy, Scr. Mater. 115 (2016) 150–154.
[3] W. Chominski, M. Lewandowska, Precipitation phenomena in ultrafine grained Al-Mg-Si alloy with heterogeneous microstructure, Acta Mater. 103 (2016) 547–557.
[4] T. Hu, J.H. Chen, J.Z. Liu, Z.R. Liu, C.L. Wu, The crystallographic and morphological evolution of the strengthening precipitates in Cu-Ni-Si alloys, Acta Mater. 61 (2013) 1210–1219.
[5] I. Markovic, S. Nestovic, B. Markoli, M. Premovic, S. Mladenovic, Study of anneal hardening in cold worked Cu-Au alloys, J. Alloys Compnd. 658 (2015) 414–421.
[6] C. Cao, D. Zhang, Z.B. He, L.Z. Zhuang, J.S. Zhang, Enhanced and accelerated age hardening response of Al-5.2Mg-0.45Cu (wt%) alloy with Zn addition, Mater. Sci. Eng. A 666 (2016) 34–42.
[7] C. Li, G. Sha, B. Gun, J.H. Xia, X.F. Liu, Y.Y. Bu, N. Birbilis, S.P. Ringer, Enhanced age-hardening response of Al-4Mf-1Cu (wt%) microalloyed with Ag and Si, Scr. Mater. 68 (2013) 857–860.
[8] P. Sahu, S.K. Pradham, M. De, X-ray diffraction studies of the decomposition and microstructural characterization of cold-worked powders of Cu-15Ni-Sn alloys, J. Alloys Compnd. 377 (2004) 103–116.
[9] V.M. López-Hirata, A.J. Arias-Pérez, M.L. Saucedo-Muñoz, A study of precipitation in Cu-15Ni-Sn alloys, J. Mater. Sci. Lett. 18 (1999) 1697–1699.
[10] T.D. Shen, C.C. Koch, Formation, solid solution hardening and softening of nanocrystalline solid solutions prepared by mechanical attrition, Acta Mater. 44 (1996) 753–761.
[11] E. Donoso, R. Espinoza, M.J. Diánez, J.M. Criado, Microcalorimetric study of the annealing hardening mechanism of a Cu-2.8Ni-1.4Si (at%) alloy, Mater. Sci. Eng. A 556 (2012) 612–616.
[12] S. Sheibani, S. Heshmati-Manesh, A. Ataie, A. Caballero, J.M. Criado, Spinodal decomposition and precipitation in Cu-Cr nanocomposite, J. Alloys Compnd. 587 (2014) 670–676.
[13] T. Klassen, U. Herr, R.S. Averback, Ball milling of systems with positive heat of mixing: effect of temperature in Ag-Cu, Acta Mater. 45 (1997) 2921–2930.
[14] M.J. Diánez, E. Donoso, J.M. Criado, M.J. Sayagués, G. Díaz, L. Olivares, Study by DSC and HRTEM of the aging strengthening of Cu-Ni-Zn-Al alloys, Mater. Des. 92 (2016) 184–188.
[15] S. Sheibani, A. Ataie, S. Heshmati-Manesh, A. Caballero, J.M. Criado, Influence of Al_2O_3 reinforcement on precipitation kinetics of Cu-Cr nanocomposites, Thermochim. Acta 526 (2011) 222–228.
[16] K. Abib, F. Hadllarby, L. Rabahi, B. Alili, D. Bradai, DSC analysis of commercial Cu-Cr-Zr alloy processed by equal channel angular pressing, Trans. Ninferreous Met. Soc. China 25 (2015) 838–843.
[17] S. Esmaeili, X. Wang, D.J. Lloyd, W.J. Poole, On the precipitation-hardening behavior of the Al-Mg-Si-Cu alloy AA6111, Metall. Mater. Trans. A 34 A (2003) 751–763.
[18] W. Raymond, M.J. Gedeon, Performances advances in copper-nickel-tin spinodal alloys, Adv. Mater. Proc. 171 (2013) 20–25.
[19] E.G. Barburaj, U.D. Kulkarni, E.S.K. Menon, R. Krishnan, Initial stages of decomposition in Cu-9Ni-6Sn, J. Appl. Cryst. 12 (1979) 476–480.
[20] L. Liu, H. Huang, R. Fu, D. Liu, T.Y. Zhang, DO_{22}-$(Cu,Ni)_3Sn$ intermetallic compound nanolayer formed in Cu/Sn-nanolayer/Ni structures, J. Alloys Compnd. 486 (2009) 207–211.
[21] J.C. Zhao, M.R. Notis, Spinodal decomposition, ordering transformation and discontinuous precipitation in a Cu-15Ni-8Sn alloy, Acta Mater. 46 (1998) 4203–4218.
[22] J.C. Rao, M.R. Notis, Microstructure and precipitation kinetics in a Cu-7.5Ni-5Sn alloy, Scr. Mater. 11 (1998) 1509–1516.
[23] J.B.B. Singh, J.G. Wen, P. Bellon, Nanoscale characterization of the transfer layer formed during dry sliding of Cu-15wt%Ni-8wt%Sn bronze alloy, Acta Mater. 56 (2008) 3053–3064.
[24] M.J. Diánez, E. Donoso, M.J. Sayagués, A. Perejón, P.E. Sánchez-Jiménez, L.A. Pérez-Maqueda, J.M. Criado, The calorimetric analysis as a tool for studying the aging hardening mechanism of a Cu-10wt%Ni-5.5wt%Sn alloy, J. Alloys Compnd. 688 (2016) 288–294.
[25] R.D.B. Frazer, E. Suzuki, Resolution of overlapping bands-functions for simulating bamd shapes Snsl, Chem 41 (1969) 37–39.
[26] A. Perejón, P.E. Sánchez-Jiménez, J.M. Criado, L.A. Pérez-Maqueda, Kinetic analysis of Complex Solid-State reactions. A new deconvolution procedure, J. Phys. Chem. B 115 (2011) 1780–1791.
[27] R. Svoboda, J. Málek, Applicability of Fraser-Suzuki function in kinetic analysis of complex crystallization processes, J. Therm. Anal. Calorim. 111 (2013) 1045–1056.
[28] H.G. Kim, S.Z. Han, K. Euh, S.H. Lim, Effects of C addition and thermo-mechanical treatment on microstructures and properties of Cu-Fe-P alloys, Mater. Sci. Eng. A 530 (2011) 652–658.
[29] J.H. Kim, J.H. Jeun, H.J. Chun, Y.R. Lee, J.T. Yoo, J.H. Yoon, H.S. Lee, Effect of precipitates on mechanical properties of AA2195, J. Alloys Compnd. 669 (2016) 187–198.
[30] E. Donoso, G. Díaz, J.M. Criado, Kinetics analysis of precipitation in a quasi-binary Cu-1 at% CoTo alloy, J. Therm. Anal. Calorim. 91 (2008) 491–495.